Dinuclear silver(I) complexes for the design of metal–ligand networks based on triazolopyrimidines†

Ana B. Caballero,[a,b] Jana K. Maclaren,[b] Antonio Rodríguez-Diéguez,[a] Isaac Vidal,[d] Jose A. Dobado,[d] Juan M. Salas*[a] and Christoph Janiak*[b,c]

Silver(I) coordination complexes with the versatile and biomimetic ligands 1,2,4-triazolo[1,5-*a*]pyrimidine (tp), 5,7-dimethyl-1,2,4-triazolo[1,5-*a*]pyrimidine (dmtp) and 7-amine-1,2,4-triazolo[1,5-*a*]pyrimidine (7atp) all feature dinuclear $[Ag_2(\mu\text{-tp})_2]^{2+}$ building units (where tp is a triazolopyrimidine derivative), which are the preferred motif, independently of the counter-anion used. According to AIM (atoms in molecules) and ELF (electron localization function) analyses, this fact is due to the great stability of these dinuclear species. The complexes structures range from the dinuclear entities $[Ag_2(\mu\text{-tp})_2(CH_3CN)_4](BF_4)_2$ (**1**), $[Ag_2(\mu\text{-tp})_2(CH_3CN)_4](ClO_4)_2$ (**2**), $[Ag_2(\mu\text{-7atp})_2](ClO_4)_2$ (**3**) and $[Ag_2(\mu\text{-dmtp})_2(CH_3CN)](PF_6)(ClO_4)$ (**4**) over the 1D polymer chain $[Ag_2(\mu\text{-CF}_3SO_3)_2(\mu\text{-dmtp})_2]_n$ (**5**) to the 3D net $\{[Ag_2(\mu_3\text{-tp})_2](PF_6)_2 \cdot {\sim}6H_2O\}_n$ (**6**) with NbO topology.

Introduction

There is a still increasing interest in the design of extended coordination frameworks such as metal–organic frameworks (MOFs)[1] for their potential zeolitic, guest molecule absorption/storage,[2] gas separation,[3] catalytic,[4] magnetic, conducting, nonlinear optical *etc.* properties, in addition to their intriguing topologies.[5] The most common and controlled strategy to prepare metal–ligand networks consists of the self-assembly of specifically designed precursors or building blocks to generate multidimensional compounds. Therefore, there is a great interest in the search for bridging ligands, which can produce new materials with intriguing structures and novel properties. 1,2,4-triazolo[1,5-*a*]pyrimidine derivatives are ligands that display a great versatility in their interactions with metal ions,[6] giving rise in some cases to compounds with interesting metal–metal interactions.[7] Moreover, 1,2,4-triazolo[1,5-*a*]pyrimidine derivatives have been the subject of chemical and biological studies due to their pharmacology including antipyretic,

[a]Departamento de Química Inorgánica, Universidad de Granada, Severo Ochoa s/n, E-18071, Granada, Spain. E-mail: jsalas@ugr.es; Tel: 0034958248525
[b]Institut für Anorganische und Analytische Chemie, Universität Freiburg, Albertstr., 21, D-79104, Freiburg, Germany
[c]New address: Institut für Anorganische und Strukturchemie, Universität Düsseldorf, Universitätsstr., 1, D-40225, Düsseldorf, Germany. E-mail: janiak@uni-duesseldorf.de; Tel: +49-211-8112286
[d]Grupo de Modelización y Diseño Molecular. Departamento de Química Orgánica, Universidad de Granada, Severo Ochoa s/n, E-18071, Granada, Spain

analgesic, antiinflammatory, potential herbicidal, fungicidal, and leishmanicidal properties.[8] Due to these biological properties, a wide variety of their metal complexes have shown biological activity, with particular antiparasite[9] and antitumor activity.[10]

The Ag(I) ion is regarded as a soft acid that favors the coordination of soft bases, such as ligands that contain sulphur and unsaturated nitrogen atoms.[11] Complexes of silver(I) and N-heterocyclic ligands lead to the production of interesting geometric configurations and photophysical properties[12] also as coordination polymers.[13,14] However, no three-dimensional framework containing a triazolopyrimidine ligand has been reported up to now. The basic structural unit in most silver complexes containing 1,2,4-triazolo[1,5-*a*]pyrimidine- (tp-) type ligands is an $[Ag_2(\mu\text{-tp})_2]^{2+}$ eight-membered ring (Scheme 2) generated by the coordination of two triazolopyrimidine moieties to two silver atoms through the nitrogen atoms in positions 3 and 4.[15]
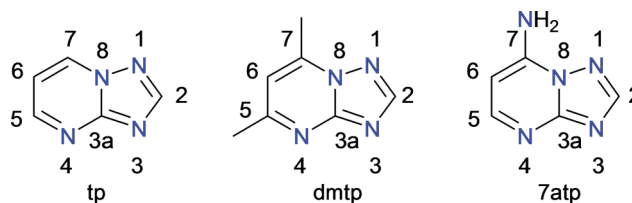
Scheme 1 1,2,4-Triazolo[1,5-*a*]pyrimidine (tp) derivatives employed.

This led to our study on the synthesis of new metal–ligand networks using the $[Ag_2(\mu\text{-tp})_2]^{2+}$ ring as secondary building unit (SBU). Due to the flexible coordination numbers of the Ag(I) ion varying from two to six, the dinuclear building-blocks could be linked through a third coordination position of the triazolopyrimidine ligand, giving extended networks.
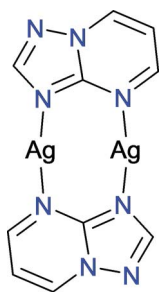
Scheme 2 Eight-membered ring $Ag_2(\mu\text{-tp})_2$ dimeric building motif.

Our aim is to develop Ag(I)-based cationic coordination networks with biomimetic ligands such as triazolopyrimidine derivatives. Recently, cationic Ag(I)-MOFs are fulfilling their potential applications as drug carriers,[16] for selective anion exchange,[17] or as catalysts.[17,18]

In this paper, we report the syntheses and structures of six novel Ag(I) compounds with the unsubstituted 1,2,4-triazolo[1,5-*a*]pyrimidine (tp), its dimethylated derivative at 5 and 7 positions (dmtp), and with an amine group at the 7 position (7atp) as ligands (Scheme 1 and Scheme 3) and we analyse the influence of the tp ligand and the counter anion on their structures. Moreover, these structural features are discussed on the basis of atoms in molecules (AIM) theory and ELF analyses, which proved to be useful tools to get a deeper knowledge about chemical bonding.
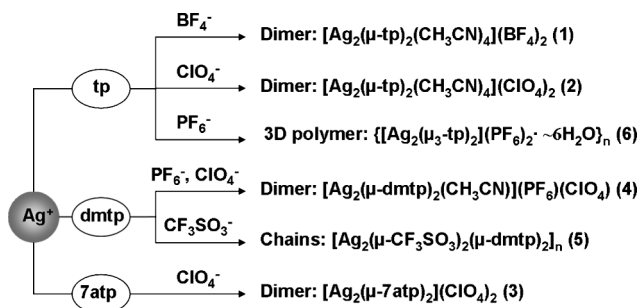
Scheme 3 Silver(I) complexes obtained with tp, dmtp and 7atp ligands.

Results and discussion

The silver-tp, -dmtp and -7atp compounds **1–6** (Scheme 3) are prepared in darkness in good to high yield as colorless crystals by the reaction of the ligand with the silver salt in acetonitrile solution. In order to reach a maximum Ag coordination by the tp-nitrogen donor atoms a weakly coordinating counter anion was chosen with the silver salt.

Spectroscopic (IR spectra) and thermal properties

The 1500–1700 cm^{-1} region of the infrared spectra of the free heterocycles displays three characteristic bands for tp (1621, 1534 and 1515 cm^{-1}), two for dmtp (1638 and 1548 cm^{-1}) and three for 7atp (1680, 1656 and 1573 cm^{-1}),[19,20] which are slightly affected by the silver coordination.

The presence of the anions is indicated by the typical stretching vibrations of tetrafluoroborate (1037 cm^{-1}) in **1**, perchlorate

(1081 cm^{-1} in **2**, 1083, 1086 cm^{-1} in **3**, and 1027 cm^{-1} in **4**), hexafluorophosphate (832 cm^{-1}) in **4** and **6** and triflate (1141, 1170 and 1025 cm^{-1}) in **5**.

The first step of the thermal decomposition of complexes **1**, **2** and **4** is the loss of the acetonitrile solvent molecules. Their respective thermogravimetric diagrams (see Fig. S1 in ESI†) display well-defined weight losses in a single-step in the range 60–110 °C for **1** and **2**, and in the range 150–180 °C for **4**. The pyrolysis of the organic triazolopyrimidine moiety occurs in several steps and begins around 300 °C for all compounds. In the case of the polymeric complex **6**, dehydration begins at room temperature so its TG and DSC diagrams (see Fig. S1 in ESI†) were recorded immediately after taking crystals out of the solution. The percentage of weight loss is in good agreement with four water molecules per dimeric unit (8.87%). Immediately after dehydration, an exothermic effect appears at 177 °C, which probably indicates a structural change invoked by the loss of the water molecules embedded in the structure ($\Delta H = +16.4$ kJ mol^{-1}).

Crystal structures

Compounds **1** and **2** with the 1,2,4-triazolo[1,5-*a*]pyrimidine (tp) ligand are isostructural. Both compounds feature a molecular dinuclear cationic unit where the silver atom is coordinated by the triazole-N3, the pyrimidine-N4 and two acetonitrile nitrogen atoms in a distorted tetrahedral geometry (Fig. 1). The dinuclear units are situated around an inversion center. Despite the presence of ligand π-systems in **1** and **2** there are no intermolecular π–π or C–H···π interactions evident.[21,22] Tables for supramolecular Ag···π,[13,23] C–H···F[24] and C–H···N-interactions[25] are given in the ESI† (Table S1 and S2). As a note of caution: In view of strong Coulomb forces in the packing of the silver-ligated cation and BF$_4$ anion (Fig. S2 in ESI†) the weak supramolecular interactions should not be over-interpreted.

In compound **3** with the 7-amine-1,2,4-triazolo[1,5-*a*]pyrimidine (7atp) ligand the dinuclear cationic unit contains essentially two-coordinated Ag atoms. There is only one additional weak coordination to a perchlorate anion (Ag···OClO$_3$ 2.710(6) Å) (Fig. 2). The silver atom is again part of Ag···π interactions, the amine group enters into charge-assisted[26] H-bonds to ClO$_4^-$ (Table S3 in ESI†).

Compound **4** with the 5,7-dimethyl-1,2,4-triazolo[1,5-*a*]pyrimidine (dmtp) ligand exhibits a special dinuclear cationic unit which is not centrosymmetric and contains two different Ag atoms (Fig. 3). Ag1 is coordinated by two triazolo-N3 atoms, Ag2 is coordinated by two pyrimidine-N4 atoms. The mixed-anion composition with one perchlorate and one hexafluorophosphate anion is apparently responsible for this peculiar coordination. In addition, Ag2 binds an acetonitrile group and both Ag1 and Ag2 have a weak perchlorate interaction (Ag1···O2^{vii} 2.917(7), Ag1···O4^{vii} 2.930(6), Ag2···O2 2.752(9) Å). The Ag1-perchlorate interaction together with a sizable π–π and Ag···π stacking assembles two dinuclear Ag$_2$(μ-dmtp)$_2$ cations on top of each other (*cf*. Fig. 3, bottom). The slightly tilted triazolo rings of the stacked adjacent rings interact with a short centroid–centroid contact (3.503(4) Å) and small slip angles ($\beta = 20.52°$, $\gamma = 15.71°$) (Table S4 and Fig. S5 in ESI†). Strong π-stacking shows rather short centroid–centroid contacts (Cg···Cg < 3.8 Å) and small
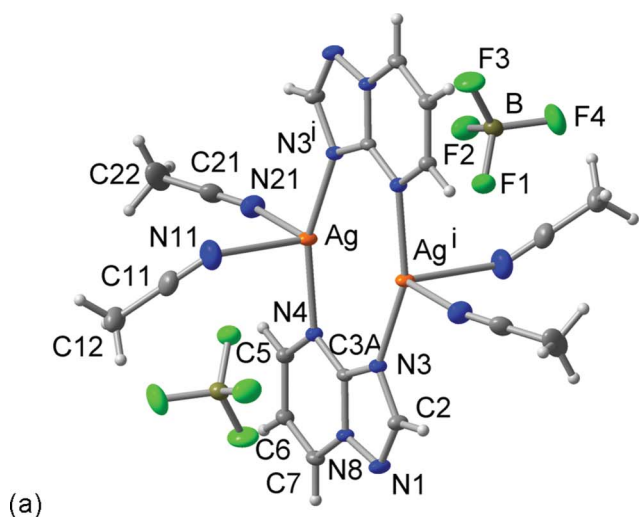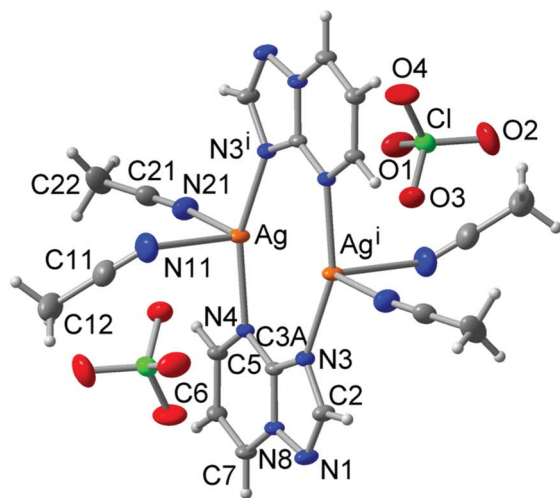
Fig. 1 Molecular dinuclear unit of (a) **1** and (b) **2** (50% probability ellipsoids). Selected bond distances and angles are given in Table 1. Symmetry transformation i = 2 − x, 1 − y, 1 − z.

Fig. 2 Molecular dinuclear unit of **3** (50% probability ellipsoids). Selected bond distances and angles are given in Table 1. Symmetry transformation ii = 1 − x, 1 − y, 1 − z.

slip angles (β, γ < 25°) which translate into a sizable overlap of the aromatic planes.[27,21]

In compound **5** the dmtp ligand also gives rise to a dinuclear silver-ligand building unit (Fig. 4). Instead of solvent molecules, two bridging triflate ligands now coordinate to the silver atom. It should be noted that the Ag···O$_{triflate}$ contacts in **5** are around 2.6 Å (Table 1) and much shorter than the Ag···O$_{perchlorate}$ contacts in **4**. Thereby parallel strands along the *a* axis are formed (Fig. 4, bottom). Neighboring strands interact with exactly parallel (by symmetry) pyrimidine rings through strong π-stacking with a rather short centroid-centroid contact (3.5290(10) Å), small slip angles (β, γ = 20.42°) and small vertical displacement (slippage, 1.231 Å) which translate into a good overlap of the aromatic planes along the C6 atom here (Fig. S6 in ESI†).[21,27]

Compound **6** is a polymeric Ag-triazolopyrimidine network. This is traced to the use of water instead of acetonitrile as the solvent. The tp ligand bridges between three symmetry related silver atoms using all its triazole-N1 and -N3 and the pyrimidine-N4 donor atoms (Fig. 5). This is the first time that a tp ligand
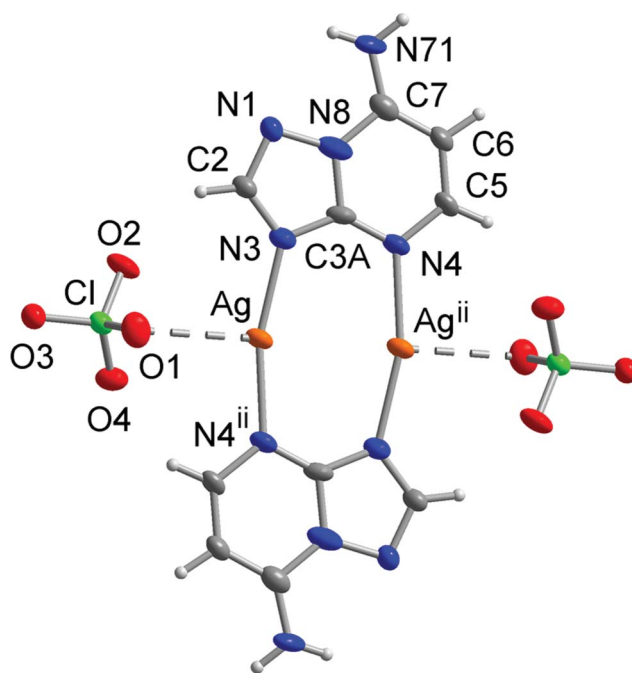
exhibits the tridentate binding mode, which is unique to this structure. Thus, the common dinuclear silver-ligand building unit is further connected to a 3D network (Fig. 6). Each silver atom is coordinated by the three different nitrogen donor atoms (Fig. 5). The Ag-triazole-N1 bond length is slightly longer (2.414 Å) than the usual Ag-N4 and -N3 distances and resembles more an Ag-*N*-acetonitrile bond in terms of distance (*cf.* Table 1). Furthermore, there is a weak Ag···F contact with a PF$_6$ anion and a water molecule of crystallization interacts on average with each eighth Ag atom, giving an oxygen occupation factor of 0.12. This aqua ligand is part of the disordered water of crystallization which occupies the channels along the threefold rotation axis parallel to the *c* axis (*cf.* Fig. 6).

The projection onto the *ab*-plane of the 3D net of **6** in Fig. 6 incorrectly looks like a Kagomé net. The topological type of this 3D net, however, is niobium oxide[28–30] or sqc35 with the point symbol (6⁴.8²)[31] as analyzed by the program package TOPOS (vertex symbol [6(2).6(2).6(2).6(2).8(2).8(2)]).[32] The NbO structure is a simple structure commonly used as model to describe more complex 3D networks and is described as an unique variant of the rock-salt NaCl structure in which there are vacancies (Nb) at the eight corners of the unit cell and an O vacancy at its centre.[33] For this topological analysis the midpoint of the Ag···Ag unit which is also the crystallographic inversion center was taken as the node and abbreviated as Sc in Fig. 7.

In the structures of **1–6** a relatively short Ag–Ag contact[34,35] is generated by the bridging action of the ligand in the eight-membered [Ag$_2$(μ-tp)$_2$]²⁺ ring (*cf.* Scheme 2). The interaction between the metal centers has been examined previously by means of *ab initio* MO calculations and the quantum theory of atoms in molecules (AIM), stating the stabilizing nature of the interaction and small covalent character of the Ag–Ag interaction.[36]

Table 1 Selected bond distances (Å) and angles (°) in **1–6**[a]

	1	**2**	**3**	**4**[b]
Ag–N3$_{triazolo}$	i 2.1786(12)	i 2.1845(16)	2.126(4)	2.141(4) / 2.124(4)
Ag–N4$_{pyrimdin}$	2.2281(12)	2.2339(15)	ii 2.137(4)	2.241(4) / 2.227(4)
Ag–N11$_{NCMe}$	2.5127(16)	2.520(2)	—	Ag2–N9$_{NCMe}$ 2.371(6)
Ag–N21$_{NCMe}$	2.4393(15)	2.436(2)	—	—
Ag···Ag	i 3.0868(4)	i 3.0987(5)	ii 2.9549(10)	2.9852(10)
Ag···O	—	—	2.710(6)	vii 2.917(7)[c] / vii 2.930(6)[c] / 2.752(9)
N3$_{tri}$–Ag–N4	i 159.12(5)	i 158.63(6)	ii 164.43(18)	163.84(15)[d] / 160.78(14)[e]
N3$_{tri}$–Ag–N21	i 102.45(5)	i 103.05(7)	—	—
N4$_{py}$–Ag–N21	92.84(5)	92.94(7)	—	95.83(18)[e] / 103.04(18)[e]
N3$_{tri}$–Ag–N11	i 98.93(6)	i 97.48(8)	—	—
N4$_{py}$–Ag–N11	94.71(6)	95.62(8)	—	—
N21–Ag–N11	91.59(6)	93.32(9)	—	—

	5		**6**
Ag–N3$_{triazolo}$	ii 2.1839(14)		ii 2.1830(16)
Ag–N4$_{pyrimidin}$	2.2277(13)		2.2151(17)
Ag–O11^{ii}	2.5598(13)	Ag–N1^{ix}	2.4136(19)
Ag–O12	2.6081(13)	Ag–O1W	2.218(19)
Ag–Ag^{ii}	3.0398(4)	Ag–Ag^{ii}	3.0015(3)
		Ag–F	2.843(3)
N3^{ii}–Ag–N4	155.91(5)	N3^{ii}–Ag–N4	158.13(7)
N3^{ii}–Ag–O11^{iii}	88.87(5)	N3^{ii}–Ag–N1^{ix}	96.03(7)
N4–Ag–O11^{iii}	110.23(5)	N4–Ag–N1^{ix}	104.59(7)
N3^{ii}–Ag–O12	110.30(5)	N3^{ii}–Ag–O1W	94.0(5)
N4–Ag O12	84.81(5)	N4–Ag–O1W	92.4(5)
O11^{iii}–Ag–O12	90.68(4)		

[a] Symmetry transformations: i = 2 − x, 1 − y, 1 − z; ii = 1 − x, 1 − y, 1 − z; iii = −x, 1 − y, 1 − z; vii = 1 − x, −y, 1 − z; ix = −1/3 + y, 1/3 − x + y, 4/3 − z. [b] Two different silver atoms (Ag1 and Ag2) in the dimeric cationic unit, which differ in only triazolo-N coordination to Ag1 and only pyrimidin-N coordination to Ag2. [c] See text for Ag···O assignment. [d] N3$_{tri}$–Ag–N13$_{tri}$. [e] N4$_{py}$–Ag–N14$_{py}$ or N4/14$_{py}$–Ag–N9$_{NCMe}$, respectively.

AIM and ELF analyses

The AIM and ELF analyses are used in order to achieve a deeper understanding of the formation of the dinuclear [Ag$_2$(μ-tp)$_2$]$^{2+}$ building units and investigate the role played by the triazolopyrimidine substituents on a three-dimensional polymer. From the AIM and ELF analyses the mechanism of the MOF-network formation may be divided in two steps, one in which the Ag(I) ion is interacting with the ligands forming the metal complexes with tp, dmtp and 7atp, and the other one in which each complex is coordinated with another one through the N1 atom.

Step one: Formation of the Ag dimeric complexes

In Table 2 are summarized the AIM atomic charges of the isolated ligands and within the complex. This information helps to follow the formation of the complex from the isolated ligand. From this data, it can be observed that the complex formation leads to an increase of the negative charge for N atoms except for N1 (meaning that the number of electrons of these atoms has increased), whereas for C atoms there is an increase of the positive charge except for C5 (meaning that the number of electrons of

Table 2 AIM atomic charges of the free ligands as obtained from the integration of the electronic density in each basin. Atoms labelling corresponds to Scheme 1

	tp	Ag$_2$(μ-tp)$_2$ complex	dmtp	Ag$_2$(μ-dmtp)$_2$ complex	7atp	Ag$_2$(μ-7atp)$_2$ complex
C2	1.03	1.14	1.03	1.16	1.02	1.16
C3a	1.39	1.61	1.39	1.62	1.39	1.62
C5	0.61	0.63	0.62	0.62	0.6	0.59
C6	−0.02	0.00	−0.05	−0.03	−0.04	−0.03
C7	0.46	0.48	0.46	0.5	0.99	1.16
N1	−0.68	−0.66	−0.70	−0.69	−0.71	−0.72
N3	−1.11	−1.36	−1.11	−1.36	−1.11	−1.34
N4	−1.16	−1.36	−1.17	−1.37	−1.15	−1.36
N8	−0.87	−0.96	−0.87	−0.96	−0.89	−0.96
Ag	—	0.79	—	0.77	—	0.88

these atoms has decreased), but these charge variations for C and N atoms are not in the same range. The populations of N3 and N4 atoms, which are connected to the Ag atoms, increase by 0.20 e⁻, whereas the population of the Ag atoms decreases by around 0.80 e⁻. Also, C atoms bonded to N atoms suffer a decrease in their electronic populations, the C3a atom being the most affected due to its binding to three N atoms. As a result of the electronic rearrangement that occurs in the dimeric complex
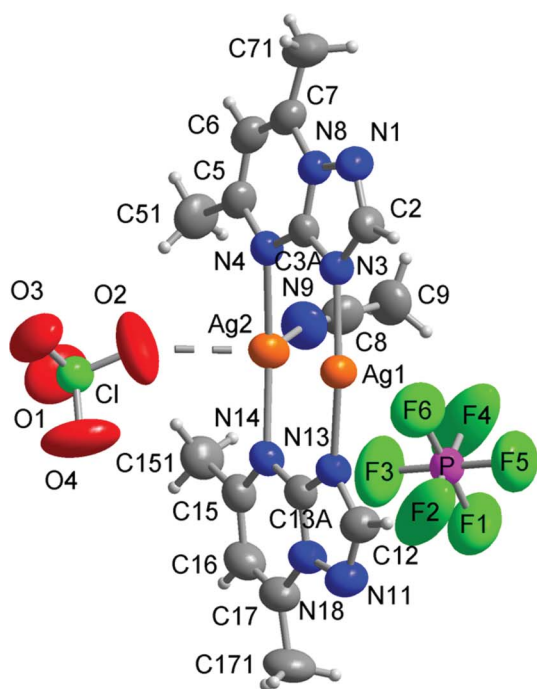
Fig. 4 Top: Molecular dinuclear unit of **5** (50% probability ellipsoids) with indication of the cation-anion strand through the triflate bridges. Bottom: Silver-triflate strands along the *a* axis. Selected bond distances and angles are given in Table 1. Symmetry transformation: ii = 1 − *x*, 1 − *y*, 1 − *z*; iii = −*x*, 1 − *y*, 1 − *z*.

Fig. 3 Top: Molecular dinuclear unit of **4** (50% probability ellipsoids). Bottom: Section of the packing in **4**. Selected bond distances and angles are given in Table 1. Symmetry transformation: vii = 1 − *x*, −*y*, 1 − *z*.
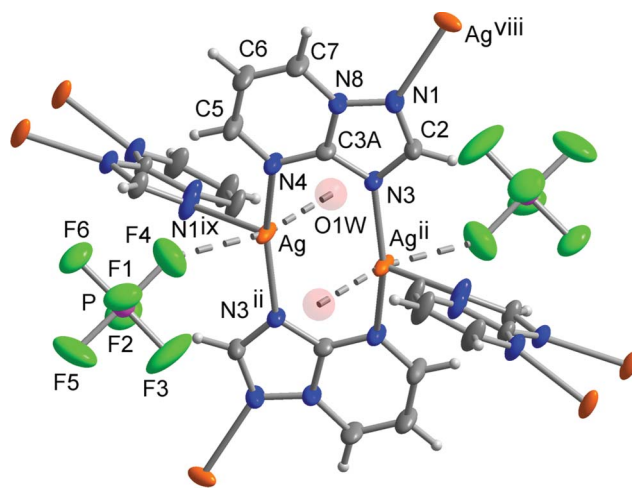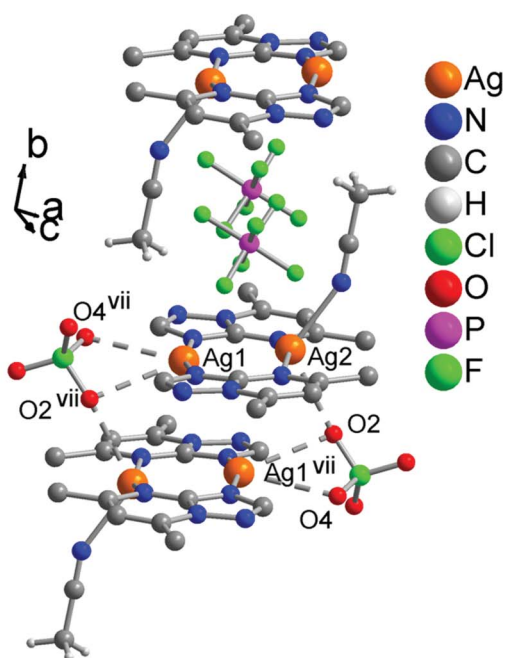
Fig. 5 Building unit of **6** with the silver coordination environment and the ligand bridging action (50% probability ellipsoids). The partially occupied oxygen atom of the aqua ligand is shown transparent. Selected bond distances and angles are given in Table 1. Symmetry transformation: ii = 1 − *x*, 1 − *y*, 1 − *z*; viii = 2/3 + *x* − *y*, 1/3 + *x*, 4/3 − *z*; ix = −1/3 + *y*, 1/3 − *x* + *y*, 4/3 − *z*.

formation, the Ag atoms have a positive charge that in order to obtain a stable complex must be neutralized. Because each Ag atom has a coordination number of two, it is still possible that the remaining two coordination positions are occupied by solvent or counter-anion molecules, yielding the formation of the complexes.

Moreover, the electronic rearrangement stated before is followed by the formation of an intramolecular chemical bond between the Ag atoms. This bond is revealed by the presence of a bond
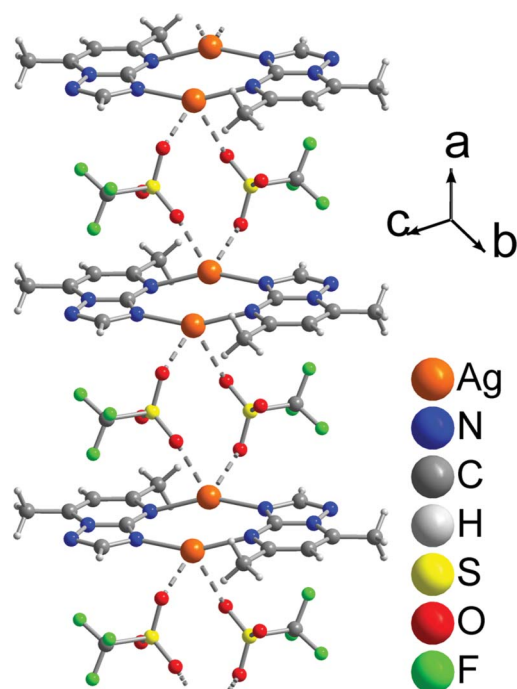
critical point bcp between the Ag atoms (Fig. S8 in ESI†). This kind of interaction was reported some years ago,[36] leading to the conclusion that this "bcp" reflects the direct interaction between the Ag atoms. Further details about the nature of such intermetallic interactions in dinuclear silver(I) complexes 1,2,4-triazol[1,5-a]pyrimidines have been reported previously by Molina *et al.*[36]

Fig. 6 Projection of the 3D network of **6** onto the *ab*-plane to illustrate the hexagonal channels parallel to the *c* axis around the threefold rotation axes. The PF$_6$ anion and the water of crystallization in the channels are not shown.
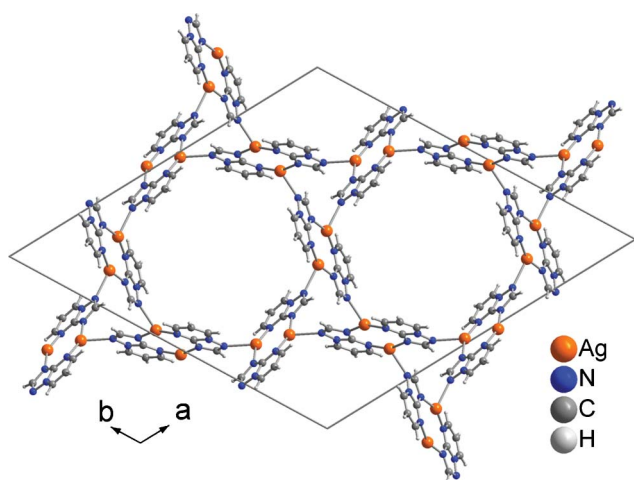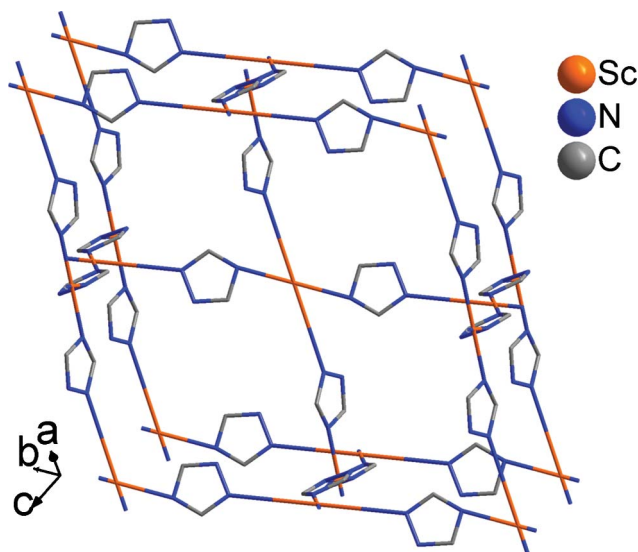

Fig. 7 Simplified net representation of **6** with the Ag···Ag midpoint (Sc) as the node. Only the triazole ring of the ligand is shown for clarity and the Sc-node connected to N3 and N1 (for further simplified net representations of **6** see Fig. S7 in the ESI†).

Step two: Formation of the 3D network

Once the Ag dinuclear complexes are formed, extended networks should be obtained by the coordination at the N1 atom with the Ag atom of other complexes.

From the ELF analysis, this process consists of the formation of a disynaptic basin between the N1 atom of one complex and the Ag atoms of another complex. The mechanism through which this disynaptic basin is formed should be similar to the formation of the N3 and N4 basins with Ag, within the dinuclear Ag–Ag complex, because the same chemical elements are involved. This mechanism depends on the electronic and geometrical conditions.

From the electronic point of view, it should be noted that, in general, AIM and ELF analyses describe "metal-to-non metal"

interactions as very polarized bonds, almost ionic, the electronic density being mainly at the non-metal atom. So, it is expected that when the 3D network is formed (the N1 atoms of one complex must form a chemical bond with the Ag atom of another complex), the Ag atom transfers some electronic charge to the N1 one, changing the electronic population of both (see Table 2). Thus, due to the ionic character of this interaction, its strength will depend on the amount of charge transfer from Ag to N1. On this basis, since the amount of charge transfer from Ag atom to N atoms follows the trend N3 > N4 > N1, the preferred coordination positions of this ligand will have the same order.

The network formation is determined by the steric hindering (Fig. 8) of the electron pairing of the N1 atom by the substituent at C7. This effect is clearly observed in the ELF analyses of the complexes, that show more or less the same topology (Fig. 9). It is remarkable that the N1 atom has a monosynaptic basin (red color) that corresponds to an unshared electron pair. This pair is shared later with another complex to form the metal–ligand network. So, if this pair is hindered by a substituent at C7 (what is clearly observed in the pictures of dmtp, 7atp), the formation of the 3D-network is impeded. Even when there is no steric hindrance, a network formation is not so straightforward with the tp ligands as can be seen in the structures of **1** and **2** and many other tp-metal structures.
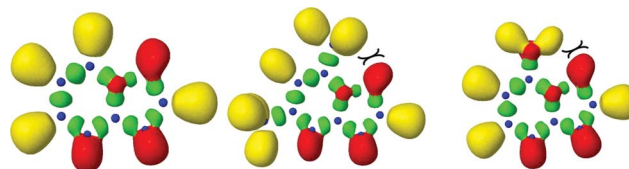

Fig. 8 ELF isosurfaces for tp, dmtp and 7atp ligands computed at a value of 0.75. The color convention represents core basins in blue, and the remaining valence basins are classified depending on the number of connections to core nuclear basins (synaptic order): red for monosynaptic, green for disynaptic and yellow for disynaptic hydrogenated basins. For dmtp and 7atp the zone hindered by the presence of a substituent at C7 is also signaled. (See Table S6 in ESI† for the values of the electronic basin populations).

Conclusions

Six new silver(I) coordination complexes with the versatile and biomimetic ligands 1,2,4-triazolo[1,5-*a*]pyrimidine (tp), 5,7-dimethyl-1,2,4-triazolo[1,5-*a*]pyrimidine (dmtp) and 7-amine-1,2,4-triazolo[1,5-*a*]pyrimidine (7atp) have been synthesized and characterized in this work. Dinuclear [Ag$_2$(μ-tp)$_2$]$^{2+}$ building units are featured in all complexes, independently of the counterion used. While these dimers are present as discrete entities in compounds **1–4**, in the case of compounds **5** and **6**, these species are connected to each other leading to 1D and 3D polymers, respectively. Compound **6** shows the capability of these dinuclear building units to form a cationic 3D silver(I) metal–ligand network with NbO topology. ELF analyses indicate that the network formation should only be possible for the unsubstituted tp derivative and strongly disfavoured by the steric hindrance from the substituent at C7 in the triazolopyrimidine ligands dmtp and 7atp.
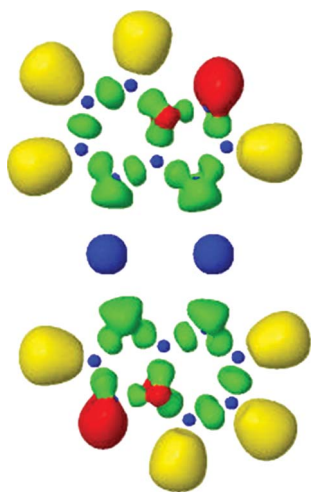
Fig. 9 ELF isosurfaces for tp complex computed at a value of 0.75. The color convention represents core basins in blue, and the remaining valence basins are classified depending on the number of connections to core nuclear basins (synaptic order): red for monosynaptic, green for disynaptic and yellow for disynaptic hydrogenated basins. (See Table S6 in ESI† for the values of the electronic basin populations).

These results open a new approach for the design and synthesis of novel porous metal–organic frameworks based on biologically relevant ligands such as 1,2,4-triazolo[1,5-*a*]pyrimidines.

Experimental section

All analytical reagents were purchased from commercial sources and used without further purification. Elemental analyses were carried out at the "Centro de Instrumentación Científica" (University of Granada) on a Fisons-Carlo Erba analyzer model EA 1108. The IR spectra on powdered samples were recorded with a ThermoNicolet IR200FTIR using KBr pellets. *Caution!* Perchlorate salts of metal complexes are potentially explosive and should be handled with extreme caution and only in very small quantities.

Preparation of [Ag₂(μ-tp)₂(CH₃CN)₄](BF₄)₂ (1) and [Ag₂(μ-tp)₂(CH₃CN)₄](ClO₄)₂ (2)

A mixture of tp (0.048 g, 0.40 mmol) and 0.40 mmol of the respective silver salt (AgBF₄ for **1**, 0.078 g; AgClO₄·H₂O for **2**, 0.083 g) in 30 mL of acetonitrile was heated to 80 °C for 30 min in darkness. The resulting clear colorless solution was kept standing at room temperature in darkness. After 3–4 days, colorless prismatic crystals suitable for XRD measurements were isolated. Yields: 27 and 66% for **1** and **2**, respectively.

Calcd. for $C_{10}H_8Ag_2B_2F_8N_8 \cdot 4CH_3CN$ (**1**): C 27.24, H 2.54, N 21.17. Found: C 26.39, H 2.35, N 20.80.

Calcd. for $C_{10}H_8Ag_2Cl_2N_8O_8 \cdot 4CH_3CN$ (**2**): C 26.40, H 2.46, N 20.52. Calcd. for $C_{10}H_8Ag_2Cl_2N_8O_8 \cdot CH_3CN$: C 20.71, H 1.59, N 18.11. Found: C 20.65, H 1.61, N 17.56.

The crystals of **2** lose the acetonitrile solvent of crystallization quickly. Therefore, the elemental analysis data corresponds to [Ag₂(tp)₂(CH₃CN)](ClO₄)₂ instead of the title compound. The yield is also referred to as the mass of [Ag₂(tp)₂(CH₃CN)](ClO₄)₂.

Main IR bands of **1**: 1623s (ν_{tp}), 1558s (ν_{py1}), 1523s (ν_{py2}), 1037vs (ν_{BF4}).

Main IR bands of **2**: 1621s (ν_{tp}), 1554s (ν_{py1}), 1523s (ν_{py2}), 1081vs (ν_{ClO4}).

Preparation of [Ag₂(μ-7atp)₂](ClO₄)₂ (3)

An aqueous solution of 7atp ligand (0.4 mmol, 0.541 g, 15 mL) was gently poured over an aqueous solution of AgClO₄·H₂O (0.4 mmol, 0.083 g, 5 mL) and the resulting clear yellow mixture was heated to 80 °C for 30 min in darkness. A few hours after keeping the solution cooling at room temperature, yellow prismatic crystals of **3** suitable for XRD analysis were isolated. Yield: 82%.

Calcd for $C_{10}H_{10}Ag_2Cl_2N_{10}O_8$: C 17.54, H 1.47, N 20.45. Found: C 17.45, H 1.57, N 19.49.

Main IR bands of **3**: 1655s (ν_{tp}), 1578s (ν_{py}), 1086vs (ν_{ClO4}).

Preparation of [Ag₂(μ-dmtp)₂(CH₃CN)](PF₆)(ClO₄) (4)

A mixture of dmtp ligand (0.40 mmol, 0.059 g), AgPF₆ (0.40 mmol, 0.101 g) and NaClO₄ monohydrate (0.4 mmol, 0.056 g) in acetonitrile (20 mL) was heated to 80 °C for 30 min in darkness. The resulting clear colorless solution was left standing at 4 °C in darkness. After one week, colorless prismatic crystals suitable for XRD measurements were isolated. Yield 72%. Calcd for $C_{16}H_{19}Ag_2ClF_6N_9O_4P$ (**4**): C 24.10, H 2.40, N 15.81. Found: C 24.08, H 2.63, N 15.07.

Main IR bands of **4**: 1631s (ν_{tp}), 1558s (ν_{py}), 1083vs (ν_{ClO4}), 832vs (ν_{PF6}).

Preparation of [Ag₂(μ-CF₃SO₃)₂(μ-dmtp)₂]ₙ (5)

A mixture of dmtp ligand (0.40 mmol, 0.059 g) and AgCF₃SO₃ (0.40 mmol, 0.103 g) in acetonitrile (30 mL) was heated to 80 °C for 30 min in darkness. The resulting clear colorless solution was left standing at room temperature and in darkness. After 3–4 days, colorless prismatic crystals suitable for XRD measurements were isolated. Yield 80%. Calcd for $C_{16}H_{16}Ag_2F_6N_8O_6S_2$: C 23.72, H 1.99, N 13.83. Found: C 23.57, H 2.26, N 13.74.

Main IR bands of **5**: 1627s (ν_{tp}), 1555s (ν_{py1}), 1246vs, 1225vs, 1140vs.

Preparation of {[Ag₂(μ₃-tp)₂](PF₆)₂ ·~6H₂O}ₙ (6)

An aqueous solution of tp ligand (0.15 mmol, 0.018 g, 15 mL) was poured over an aqueous solution of AgPF₆ (0.3 mmol, 0.076 g, 5 mL). The pale yellow mixture was slightly heated to 40 °C for 15 min in darkness. A week later, colorless prismatic crystals of **6** suitable for XRD analysis were formed. Yield 65% approx. Calcd for $C_{10}H_8Ag_2F_{12}N_8P_2$ (anhydrous) (**6**): C 16.10, H 1.08, N 15.02. Found: C 15.37, H 1.03, N 13.98. Main IR bands of **6**: 1621s (ν_{tp}), 1535s (ν_{py1}), 1516s (ν_{py2}), 831vs (ν_{PF6}).

X-ray crystal structure analysis

Suitable single crystals were carefully selected under a polarizing microscope. *Data collection*: Compound **1–3** and **5**: Rigaku R-axis Spider Image plate detector diffractometer, Mo Kα radiation (λ = 0.71073 Å), graphite monochromator, double-pass method ω-scan; data collection, cell refinement and data reduction with CrystalClear,[37] empirical (multi-scan) absorption correction with

Table 3 Crystal data and structure refinement for **1–3**

Compound	1	2	3
Empirical formula	$C_{18}H_{20}Ag_2B_2F_8N_{12}$	$C_{18}H_{20}Ag_2Cl_2N_{12}O_8$	$C_{10}H_{10}Ag_2Cl_2N_{10}O_8$
M/g mol^{-1}	793.82	819.10	684.92
Crystal size/mm	$0.20 \times 0.11 \times 0.10$	$0.21 \times 0.11 \times 0.09$	$0.32 \times 0.18 \times 0.16$
Crystal appearance	block, colorless	prism, colorless	prism, colorless
2θ range/°	6.52–66.28	6.48–82.26	4.28–50.00
h; k; l range	±9; ±16; ±17	±11; −18,19; ±21	±6; ±9; ±12
T/K	113	123	113
Crystal system	Triclinic	Triclinic	Triclinic
Space group	$P\bar{1}$	$P\bar{1}$	$P\bar{1}$
a/Å	6.2201(2)	6.32530(10)	5.7889(15)
b/Å	10.6272(2)	10.7545(2)	8.389(2)
c/Å	11.5588(8)	11.5478(8)	10.138(3)
α (°)	110.016(8)	110.093(8)	109.414(3)
β (°)	99.817(7)	100.489(7)	91.774(3)
γ (°)	91.442(6)	90.426(6)	102.566(3)
V/Å^3	704.51(6)	723.32(5)	450.4(2)
Z	1	1	1
D_c/g cm^{-3}	1.871	1.880	2.525
$F(000)$	388	404	332
μ/mm^{-1}	1.476	1.602	2.543
Max/min transmission	0.8725/0.7567	0.8692/0.7296	0.6864/0.4966
Reflections collected	33 624	73 832	4319
Indep. reflections (R_{int})	5349 (0.0330)	9586 (0.0362)	1575 (0.0306)
Obs. reflect [$I > 2\sigma(I)$]	4679	7488	1450
Parameters refined	192	192	153
Max./min. $\Delta\rho^a$/e Å^{-3}	1.392/−0.972	1.585/−1.580	1.403/−1.012
R_1, wR_2 [$I > 2\sigma(I)$]^b	0.0260/0.0445	0.0485/0.0876	0.0396/0.1014
R_1, wR_2 (all reflect.)^b	0.0333/0.0469	0.0720/0.1016	0.0434/0.1034
Goodness-of-fit on F^{2c}	1.145	1.079	1.102
Weight. scheme w; a/b^d	0.0095/0.5767	0.0299/1.5795	0.0637/0.7405

^{a} Largest difference peak and hole. ^{b} $R_1 = [\Sigma(\|F_o|-|F_c\|)/\Sigma|F_o|]$; w$R_2 = [\Sigma[w(F_o^2 - F_c^2)^2]/\Sigma[w(F_o^2)^2]]^{1/2}$. ^{c} Goodness-of-fit $= [\Sigma[w(F_o^2 - F_c^2)^2]/(n-p)]^{1/2}$. ^{d} $w = 1/[\sigma^2(F_o^2) + (aP)^2 + bP]$ where $P = (\max(F_o^2 \text{ or } 0) + 2F_c^2)/3$.

ABSCOR.[38] Compound **4** and **6**: Bruker Smart Apex CCD (with normal X-ray tube) and Bruker APEX2 CCD diffractometer (with microfocus tube), respectively, Mo Kα radiation ($\lambda = 0.71073$ Å), graphite monochromator, ω- and ϕ-scan; data collection with Apex2,[39] cell refinement and data reduction with SAINT,[39] experimental absorption correction with SADABS.[40] *Structure Analysis and Refinement*: The structures of **1**, **2**, **5** and **6** were solved by direct methods using SHELXS-97, the structures of **3** and **4** were solved by direct methods using SIR97;[41] refinement was done by full-matrix least squares on F^2 using the SHELXL-97 program suite.[42] All non-hydrogen positions were refined with anisotropic displacement parameters. Hydrogen atoms were positioned geometrically and refined using riding models with $U_{iso}(H) = 1.2U_{eq}(CH, CH_2)$ and $U_{iso}(H) = 1.5U_{eq}(CH_3)$.

The crystal water solvent in the channels of compound **6** was found highly disordered and could not be properly defined. Hence, the option SQUEEZE in PLATON for Windows[43] was used to refine the framework structure without the disordered electron density in the voids. Total solvent accessible void volume = 2244 Å^3/unit cell volume. With the expected volume for a hydrogen-bonded H_2O molecule of ~40 Å^3 this agrees with about 54 H_2O molecules per unit cell (with 18 Ag(tp) formula units) or 6 H_2O per Ag$_2$(tp)$_2$ formula unit.

Crystal data and details on the structure refinement are given in Table 3 and 4. Graphics were drawn with DIAMOND,[44] analyses on the supramolecular π-stacking, C–H$\cdots$N/O/F- and C–H$\cdots\pi$-interactions with PLATON for Windows.[43] The structural

data have been deposited with the Cambridge Crystallographic Data Center (CCDC No. 819202–819207).†

Computational details

Overview of the AIM theory and ELF analyses. DFT calculations, at the B3LYP[45] and M05-2X[46,47] theoretical levels, have been performed with the Gaussian09 program,[48] using the following basis sets: Ahlrichs-pVDZ[49–51] for the complexes and the 6-31+G** one[52] for the ligands (tp, dmtp, 7atp). All structures were fully optimized at the following theoretical levels: B3LYP/6-31+G**//B3LYP/6-31+G** for tp, dmtp, 7atp molecules, and M05-2X/Ahlrichs-pVDZ//M05-2X/Ahlrichs-pVDZ for the complexes. The local stability of all structures was checked through the eigenvalues of the matrix of second derivatives (Hessian); all energetic minima presented no imaginary frequencies.

The electronic structure resulting from the calculations was analyzed in terms of the AIM theory[53–55] and, complementarily, through the distribution of the electron localization function. This function was first introduced by Becke and Edgecombe[56] and reinterpreted by Silvi and Savin[57] as a measure of the excess of local kinetic energy due to Pauli's exclusion principle, in comparison to a uniform electron gas. The ELF definition, which is found elsewhere,[57] yields values between 0 and 1. Values close to 1 indicate electron pairing at that point, whereas values near 0 are usually found in regions between electron pairs. As in AIM analysis, it is possible to divide the molecular domain in basins grouped around

Table 4 Crystal data and structure refinement for **4–6**

Compound	4	5	6
Empirical formula	$C_{16}H_{19}Ag_2ClF_6N_9O_4P$	$C_8H_8AgF_3N_4O_3S$	$C_5H_{10}AgF_6N_4O_3P^e$
M/g mol^{-1}	797.56	405.11	427.01
Crystal size/mm	$0.45 \times 0.32 \times 0.20$	$0.20 \times 0.11 \times 0.10$	$0.08 \times 0.05 \times 0.05$
Crystal appearance	prism, colorless	block, colorless	block, colorless
2θ range/°	4.00–50.60	6.46–66.28	3.12–56.56
h; k; l range	±13; ±13; ±14	±12; ±13; ±13	−34,16; 0,34; 0,14
T/K	293	133	103
Crystal system	Triclinic	Triclinic	Trigonal
Space group	$P\bar{1}$	$P\bar{1}$	$R3$
a/Å	11.228(5)	8.3689(2)	26.0272(3)
b/Å	11.471(5)	8.6550(2)	26.0272(3)
c/Å	12.191(5)	9.0743(6)	11.0746(2)
α (°)	110.932(5)	93.984(7)	90
β (°)	112.874(5)	94.541(7)	90
γ (°)	97.284(5)	112.430(8)	120
V/Å^3	1285.2(10)	602.09(4)	6497.01(16)
Z	2	2	18
D_c/g cm^{-3}	2.061	2.235	1.964
$F(000)$	780	396	3744
μ/mm^{-1}	1.777	1.900	1.584
Max/min transmission	0.7176/0.5019	0.8327/0.7025	0.9250/0.8904
Reflections collected	13 078	55 683	3592
Indep. reflections (R_{int})	4676 (0.0190)	4585 (0.0353)	3592 (0.0000)
Obs. reflect [$I > 2\sigma(I)$]	3802	4237	3041
Parameters refined	357	183	159
Max./min. $\Delta\rho^a$/e Å^{-3}	0.695/−0.612	0.861/−0.681	1.065/−0.955
R_1, wR_2 [$I > 2\sigma(I)$]^b	0.0420/0.1123	0.0244/0.0532	0.0256/0.0612
R_1, wR_2 (all reflect.)^b	0.0521/0.1190	0.0270/0.0541	0.0309/0.0630
Goodness-of-fit on F^{2c}	1.048	1.165	1.066
Weight. scheme w; a/b^d	0.0646/1.1555	0.0163/0.6612	0.0296/12.7529

^{a} Largest difference peak and hole. ^{b} $R_1 = [\Sigma(\|F_o|-|F_c\|)/\Sigma|F_o|]$; w$R_2 = [\Sigma[w(F_o^2 - F_c^2)^2]/\Sigma[w(F_o^2)^2]]^{1/2}$. ^{c} Goodness-of-fit $= [\Sigma[w(F_o^2 - F_c^2)^2]/(n - p)]^{1/2}$. ^{d} $w = 1/[\sigma^2(F_o^2) + (aP)^2 + bP]$ where $P = (\max(F_o^2 \text{ or } 0) + 2F_c^2)/3$. ^{e} The majority of the 3 disordered crystal water molecules per mono-silver formula unit (54 H_2O/cell) could not be located and was "SQUEEZED out" but is included in formula, mass, density, $F(000)$, max/min transmission.

the ELF attractors. From a chemical standpoint, basins can be classified as being of core, valence, or hydrogenated. If the basin does not contain a nucleus, it is called a valence basin, whereas if it contains a nucleus other than a proton it is called a core basin, or hydrogenated if a proton is inside the basin. Valence basins are characterized by the number of core basins with which they are connected and this is known as the synaptic order.[58]

AIM data (Laplacian plot) were calculated with MORPHY98,[59] while charges were integrated with AIM2000 Software.[60] ELF was computed with ToPMoD,[58] and isosurfaces were rendered with Jmol v11.7[61] visualization package.

Notes and references

1 C. Janiak and J. K. Vieth, *New J. Chem.*, 2010, **34**, 2366–2388; C. Janiak, *Dalton Trans.*, 2003, 2781; B. Moulton and M. J. Zaworotko, *Chem. Rev.*, 2001, **34**, 319; A. Oxtoby and N. R. Champness, *Coord. Chem. Rev.*, 2003, **246**, 145; S. Kitagawa, R. Kitaura and S. I. Noro, *Angew. Chem., Int. Ed.*, 2004, **43**, 2334; M. Eddaoudi, D. B. Moler, H.-L. Li, B. Chen, T. M. Reineke, M. O'Keeffe and O. M. Yaghi, *Acc. Chem. Res.*, 2001, **34**, 319; S. Kitagawa and K. Uemura, *Chem. Soc. Rev.*, 2005, **34**, 109; G. Férey, C. Mellot-Draznieks, C. Serre and F. Millange, *Acc. Chem. Res.*, 2005, **38**, 217; S. R. Batten, *Curr. Opin. Solid State Mater. Sci.*, 2001, **5**, 107; O. R. Evans and W. Lin, *Acc. Chem. Res.*, 2002, **35**, 511; Y. García, V. Niel, M. C. Muñoz and J. A. Real, *Top. Curr. Chem.*, 2004, **233**, 229; M. Yoshizawa, T. Kusukawa, M. Kawano, T. Ohhara, I. Tanaka, K. Kurihara, N. Niimura and M. Fujita, *J. Am. Chem. Soc.*, 2005, **127**, 2798; B. Kensali and W. B. Lin, *Coord. Chem. Rev.*, 2003, **246**, 305; *Magnetism: Molecules to Materials*, ed. J. S. Miller and M. Drillon, volumes *I–V*, VCH, Weinheim, 2001–2005; E. Coronado and P. Day, *Chem. Rev.*, 2004, **104**, 5419; L. J. Murray, M. Dinca and J. R. Long, *Chem. Soc. Rev.*, 2009, **38**, 1294.
2 Y. H. Hu and L. Zhang, *Adv. Mater.*, 2010, **22**, E117.
3 Y.-S. Bae, O. K. Farha, A. M. Spokoyny, C. A. Mirkin, J. T. Hupp and R. Q. Snurr, *Chem. Commun.*, 2008, 4135; Y. S. Bae, O. K. Farha, J. T. Hupp and R. Q. Snurr, *J. Mater. Chem.*, 2009, **19**, 2131; J. An, S. J. Geib and S. N. L. Rosi, *J. Am. Chem. Soc.*, 2010, **132**, 38.
4 L. Ma, C. Abney and W. Lin, *Chem. Soc. Rev.*, 2009, **38**, 1248; J. Lee, O. K. Farha, J Roberts, K. A. Scheidt, S. T. Nguyen and J. T. Hupp, *Chem. Soc. Rev.*, 2009, **38**, 1450.
5 M. O'Keeffe, M. A. Peskov, S. J. Ramsden and O. M. Yaghi, *Acc. Chem. Res.*, 2008, **41**, 1782; G. Ferey, *Chem. Soc. Rev.*, 2008, **37**, 191.
6 J. M. Salas, M. A. Romero, M. Purificación Sánchez and M. Quirós, *Coord. Chem. Rev.*, 1999, **193–195**, 1119.
7 J. A. R. Navarro, M. A. Romero, J. M. Salas, M. Quirós and E. R. T. Tiekink, *Inorg. Chem.*, 1997, **36**, 4988; A. B. Caballero, A. Rodríguez-Diéguez, E. Barea, M. Quirós and J. M. Salas, *CrystEngComm*, 2010, **12**, 3038; A. B. Caballero, A. Rodríguez-Diéguez, L. Lezama, E. Barea and J. M. Salas, *Dalton Trans.*, 2011, **40**, 5180; H. M. Abul-Haj, M. Quirós, J. M. Salas, J. A. Dobado, J. Molina, M. G. Basallote and M. A. Máñez, *Eur. J. Inorg. Chem.*, 2002, 811; M. Abul Haj, M. Quirós, J. M. Salas and R. Faure, *J. Chem. Soc., Dalton Trans.*, 2001, 1798; M.

Abul-Haj, M. Quirós, J. M. Salas and R. Faure, *Inorg. Chem. Commun.*, 2001, **4**, 254; M. Abul Haj, M. Quirós and J. M. Salas, *J. Chem. Soc., Dalton Trans.*, 2002, 4740; J. A. R. Navarro, M. A. Romero and J. M. Salas, *J. Chem. Soc., Dalton Trans.*, 1997, 1001; N. Lekkas, N. Hadjiliadis, A. Garoufis, J. Kobe, P. V. Bernhardt and E. R. T. Tiekink, *Inorg. Chim. Acta*, 2006, **359**, 4297; M. Abul-Haj, M. Quirós and J. M. Salas, *Polyhedron*, 2004, **23**, 2373.

8 G. Fischer, *Z. Chem.*, 1990, **30**, 305; G. Fischer, *Adv. Heterocycl. Chem.*, 1993, **57**, 81; E. S. H. Elashry and N. Rashed, *Adv. Heterocycl. Chem.*, 1999, **72**, 127; Y. Makisumi, H. Watanabe and K. Tori, *Chem. Pharm. Bull.*, 1964, **12**, 204; W. W. Paudler and L. S. Helmick, *J. Heterocycl. Chem.*, 1968, **5**, 691; E. Kleinpeter, R. Borsdorf, G. Fischer and H. J. Hofmann, *J. Prakt. Chem.*, 1972, **314**, 515; T. La Noce and A. M. Giuliani, *Tetrahedron*, 1978, **34**, 2927; R. J. Pugmire, J. C. Smith, D. M. Grant, B. Stanovnik, M. Tisler and B. Vercek, *J. Heterocycl. Chem.*, 1987, **24**, 805; W. W. Paudler, R. M. Sheets and B. Goodson, *Org. Magn. Reson.*, 1982, **18**, 87; M. Kuenstlinger and E. Breitmeier, *Synthesis*, 1983, **1**, 44; L. Stefaniak, M. Witanowski, U. Mahmoud, J. D. Roberts and G. A. Webb, *J. Crystallogr. Spectrosc. Res.*, 1989, **19**, 159; J. Wiench, L. Stefaniak and G. A. Webb, *Magn. Reson. Chem.*, 1994, **32**, 373; E. Kleinpeter, S. Thomas and G. Fischer, *J. Mol. Struct.*, 1995, **355**, 27; R. Gujjar, A. Marwaha, F. El Mazouni, J. White, K. L. White, S. Creason, D. M. Shackleford, J. Baldwin, W. N. Charman, F. S. Buckner, S. Charman, P. K. Rathod and M. A. Phillips, *J. Med. Chem.*, 2009, **52**, 1864; W. Tang and D. Q. Shi, *J. Heterocycl. Chem.*, 2010, **47**, 162; Q. Chen, Z. M. Liu, C. N. Chen, L. L. Jiang and G. F. Yang, *Chem. Biodiversity*, 2009, **6**, 1254; N. A. El-Koussi, F. A. Omar, S. A. Abdel-Aziz and M. F. Radwan, *Biol. Pharm. Bull.*, 2004, **27**, 141; R. P. Srivastava, V. V. Kumar, S. Bhatia and S. Sharma, *Indian J. Chem. (Sect. B)*, 1995, **34B**, 209; E. Bakhite and A. Ghafar, *Pharmazie*, 1995, **50**, 33.

9 I. Ramírez-Macías, C. Marín, J. M. Salas, A. B. Caballero, M. J. Rosales, N. Villegas, A. Rodríguez-Dieguez, E. Barea and M. Sánchez-Moreno, *J. Antimicrob. Chemother.*, 2011, **66**, 813; C. R. Maldonado, C. Marin, F. Olmo, O. Huertas, M. Quirós, M. Sánchez-Moreno, M. J. Rosales and J. M. Salas, *J. Med. Chem.*, 2010, **53**, 6964; F. Luque, C. Fernández-Ramos, E. Entrala, M. J. Rosales, C. Marín, J. M. Salas, J. A. R. Navarro and M. Sánchez-Moreno, *Toxicol. in Vitro*, 2000, **14**, 487; F. Luque, C. Fernández-Ramos, E. Entrala, M. J. Rosales, J. A. R. Navarro, M. A. Romero, J. M. Salas and M. Sánchez-Moreno, *Comparative Biochem. and Physiol. Part C*, 2000, **126**, 39; R. Magán. C. Marín, M. J. Rosales, M. A. Barrera, J. M. Salas and M. Sánchez-Moreno, *Pharmacology*, 2004, **70**, 83; R. Magán, C Marín, M. J. Rosales, J. M. Salas and M. Sánchez-Moreno, *Pharmacology*, 2005, **73**, 41; S. Boutaleb-Charki, C Marín, C. R. Maldonado, M. J. Rosales, J. Urbano, R. Gutiérrez-Sánchez, M. Quirós, J. M. Salas and M. Sánchez-Moreno, *Drug Metab. Lett.*, 2009, **3**, 35; J. M. Salas, M. Quirós, M. Abul-Haj, R. Magán, C. Marín, M. Sánchez-Moreno and R. Faure, *Met.-Based Drugs*, 2001, **8**, 119.

10 K. Akdi, R. A. Vilaplana, S. Kamah, J. A. R. Navarro, J. M. Salas and F. González-Vílchez, *J. Inorg. Biochem.*, 2002, **90**, 51; I. Lakowska, E. Szlyk, J. Sitkowski, L. Kozerski, J. Wietrzyk, M. Pelczynska, A. Nasulewicz and A. Opolski, *J. Inorg. Biochem.*, 2004, **98**, 167; J. A. R. Navarro, J. M. Salas, M. A. Romero, R. Vilaplana, F. González-Vílchez and R. Faure, *J. Med. Chem.*, 1998, **41**, 332; I. Lakomska, *Inorg. Chim. Acta*, 2009, **362**, 669; J. Ruiz, M. D. Villa, N. Cutillas, G. López, C. de Haro, D. Bautista, V. Moreno and L. Valencia, *Inorg. Chem.*, 2008, **47**, 4490; I. Lakomska, H. Kooijman, A. L. Spek, W. Shen and J. Reedijk, *Dalton Trans.*, 2009, 10736; A. H. Velders, A. Bergamo, E. Alessio, E. Zangrando, J. G. Haasnoot, C. Casarsa, M. Cocchietto, S. Zorzet and G. Sava, *J. Med. Chem.*, 2004, **47**, 1110; N. Zhang, S. Ayral-Kaloustian, T. Nguyen, J. Afragola, R. Hernández, J. Lucas, J. Gibbons and C. Beyer, *J. Med. Chem.*, 2007, **50**, 319.

11 Y. Suenga, T. Kuroda-Sowa, M. Maekawa and M. Munakata, *J. Chem. Soc., Dalton Trans.*, 2000, 3620; M. J. Hannon, C. L. Painting and N. W. Alcock, *Chem. Commun.*, 1999, 2023; X.-H. Bu, W. Chen, W.-F. Hou, M. Du, R.-H. Zhang and F. Brisse, *Inorg. Chem.*, 2002, **41**, 3477; X. M. Ouyang, B. L. Fei, T. A. Okamura, H. W. Bu, W. Y. Sun, W. X. Tang and N. Ueyama, *Eur. J. Inorg. Chem.*, 2003, 618; A. J. Blake, R. O. Gould, W.-S Li, V. Lippolis, S. Parsons, C. Radek and M. Schröder, *Inorg. Chem.*, 1998, **37**, 5070; P. J. Blower, J. A. Clarkson, S. C. Rawle, J. A. R. Hartman, R. E. Jr. Wolf, R. Yagbasan, S. G. Bott and S. R. Cooper, *Inorg. Chem.*, 1989, **28**, 4040.

12 V. J. Catalano, H. M. Kar and J. Garnas, *Angew. Chem., Int. Ed.*, 1999, **38**, 1979; G.-Q. Zhang, G.-Q. Yang, L.-Y Yang, Q.-Q. Chen and J.

S. Ma, *Eur. J. Inorg. Chem.*, 2005, 1919; X.-C. Huang, S. L. Zheng, J. P. Zhang and X. M. Chen, *Eur. J. Inorg. Chem.*, 2004, **5**, 1024; C.-X. Ren, B.-H. Ye, F. He, L. Cheng and X.-M. Chen, *CrystEngComm*, 2004, **6**, 200; Y.-B. Dong, J.-Y. Cheng, J.-P. Ma, R.-Q. Huang and M. D. Smith, *Cryst. Growth Des.*, 2005, **5**, 585; V. J. Catalano and M. A. Malwitz, *Inorg. Chem.*, 2003, **42**, 5483; Y. Kang, C. Seward, D. Song and S. Wang, *Inorg. Chem.*, 2003, **42**, 2789; X. M. Ouyang, D. J. Liu, T. A. Okamura, H. W. Bu, W. Y. Sun, W. X. Tang and N. Ueyama, *Dalton Trans.*, 2003, 1836; V. W. W. Yam, W. Y. Lo and N. Zhu, *Chem. Commun.*, 2003, 2446; M. Munakata, L. P. Wu, T. Kuroda-Sowa, M. Maekawa, Y. Suenaga, G. L. Ning and T. Kojima, *J. Am. Chem. Soc.*, 1998, **120**, 8610; H. Schmidbaur, W. Bublak, B. Huber, G. Reber and G. Müller, *Angew. Chem., Int. Ed. Engl.*, 1986, **25**, 1089; C. M. Che, H. K. Yip, D. Li, S. M. Peng, G. H. Lee, Y. M. Wang and S. T. Liu, *J. Chem. Soc., Chem. Commun.*, 1991, 1615; C. D. Wu, H. L. Ngo and W. Lin, *Chem. Commun.*, 2004, 1588.

13 H.-P. Wu, C. Janiak, G. Rheinwald and H. Lang, *J. Chem. Soc., Dalton Trans.*, 1999, 183.

14 C.-L. Chen, B.-S. Kang and C.-Y. Su, *Aust. J. Chem.*, 2006, **59**, 3–18; C. M. Fitchett and P. J. Steel, *Aust. J. Chem.*, 2006, **59**, 19; M. B. Duriska, S. R. Batten and D. J. Price, *Aust. J. Chem.*, 2006, **59**, 26; Y.-B. Xie, J.-R. Li and X.-H. Bu, *Aust. J. Chem.*, 2006, **59**, 34; L. Cunha-Silva, R. Ahmad and M. J. Hardie, *Aust. J. Chem.*, 2006, **59**, 40; S.-L. Zheng, M.-L. Tong and X.-M. Chen, *Coord. Chem. Rev.*, 2003, **246**, 185; N. S. Oxtoby, A. J. Blake, N. R. Champness and C. Wilson, *Proc. Natl. Acad. Sci. U. S. A.*, 2002, **99**, 4905; M. Munakata, L. P. Wu and T. Kuroda-Sowa, *Adv. Inorg. Chem.*, 1999, **46**, 173–303.

15 J. M. Salas, M. A. Romero, A. Rahmani and M. Quirós, *An. Quím. Int. Ed.*, 1996, **92**, 249; J. A. R. Navarro, J. M. Salas, M. A. Romero and R. Faure, *J. Chem. Soc., Dalton Trans.*, 1998, 901.

16 R. C. Huxford, J. Della Rocca and W. Lin, *Curr. Opin. Chem. Biol.*, 2010, **14**, 262.

17 H. Fei, D. L. Rogow and S. R. J. Oliver, *J. Am. Chem. Soc.*, 2010, **132**, 7202.

18 H. Fei, L. Paw, D. L. Rogow, M. R. Bresler, Y. A. Abdollahian and S. R. J. Oliver, *Chem. Mater.*, 2010, **22**, 2027.

19 E. Szlyk, A. Grodzicki, L. Pazderski, E. Bednarek and B. Kamiénski, *Polyhedron*, 2000, **19**, 965.

20 M. J. Nowak, H. Rostkowska, L. Lapinski, J. S. Kwiatkowski and J. Leszczynski, *Spectrochim. Acta, Part A*, 1994, **50**, 1081.

21 C. Janiak, *J. Chem. Soc., Dalton Trans.*, 2000, 3885; H. W. Roesky and M. Andruh, *Coord. Chem. Rev.*, 2003, **236**, 91.

22 M. Nishio, *CrystEngComm*, 2004, **6**, 130; M. Nishio, M. Hirota and Y. Umezawa, *The CH/π interaction (Evidence, Nature and consequences)*, Wiley-VCH, 1998; Y Umezawa, S. Tsuboyama, K. Honda, J. Uzawa and M. Nishio, *Bull. Chem. Soc. Jpn.*, 1998, **71**, 1207; C. Janiak, S. Temizdemir, S. Dechert, W. Deck, F. Girgsdies, J. Heinze, M. J. Kolm, T. G. Scharmann and O. M. Zipffel, *Eur. J. Inorg. Chem.*, 2000, 1229; M. Nishio, Y. Umezawa, K. Honda, S. Tsuboyama and H. Suezawa, *CrystEngComm*, 2009, **11**, 1757.

23 O. Z. Yesilel, G. Gunay and O. Buyukgungor, *Polyhedron*, 2011, **30**, 364; E. A. Goreshnik, Z. Mazej and M. G. Mys'kiv, *J. Organomet. Chem.*, 2010, **695**, 2201; S.-Q. Zhang, J. Han and T. C. W. Mak, *Organometallics*, 2009, **28**, 2677; K. Akhbari, A. Morsali and L. G. Zhu, *J. Mol. Struct.*, 2008, **891**, 132; L. Zhao and T. C. W. Mak, *Organometallics*, 2007, **26**, 4439.

24 J. Ruiz, V. Rodríguez, C. de Haro, A. Espinosa, J. Pérez and C. Janiak, *Dalton Trans.*, 2010, **39**, 3290; E Redel, M. Fiederle and C. Janiak, *Z. Anorg. Allg. Chem.*, 2009, **635**, 1139; H. A. Habib, A. Hoffmann, H. A. Höppe, G. Steinfeld and C. Janiak, *Inorg. Chem.*, 2009, **48**, 2166; J. Ruiz, M. D. Villa, V. Rodríguez, N. Cutillas, C. Vicente, G. López and D. Bautista, *Inorg. Chem.*, 2007, **46**, 5448; G. Althoff, J. Ruiz, V. Rodríguez, G. López, J. Pérez and C. Janiak, *CrystEngComm*, 2006, **8**, 662; G. R. Desiraju and T. Steiner, The weak hydrogen bond, in *IUCr Monograph on Crystallography*, vol. 9, Oxford Science, Oxford, 1999.

25 C. Janiak and T. G. Scharmann, *Polyhedron*, 2003, **22**, 1123; G. R. Desiraju and T. Steiner, The weak hydrogen bond, in *IUCr Monograph on Crystallography*, vol. 9, Oxford Science, Oxford, 1999; G. R. Desiraju, *Acc. Chem. Res.*, 2002, **35**, 565; M. Mascal, *Chem. Commun.*, 1998, 303.

26 A.-C. Chamayou, M. A. Neelakantan, S. Thalamuthu and C. Janiak, *Inorg. Chim. Acta*, 2011, **365**, 447; F. Zhuge, B. Wu, L. Dong, J. Yang, C. Janiak, N. Tang and X.-J. Yang, *Aust. J. Chem.*, 2010, **63**, 1358; B. Gil-Hernández, H. Höppe, J. K. Vieth, J. Sanchiz and C. Janiak, *Chem. Commun.*, 2010, **46**, 8270; H. A. Habib, B. Gil-Hernández, K.

Abu-Shandi, J. Sanchiz and C. Janiak, *Polyhedron*, 2010, **29**, 2537; B. M. Drašković, G. A. Bogdanović, M. A. Neelakantan, A.-C. Chamayou, S. Thalamuthu, Y. S. Avadhut, J. Schmedt auf der Günne, S. Banerjee and C. Janiak, *Cryst. Growth Des.*, 2010, **10**, 1665; F. Zhuge, B. Wu, J. Liang, J. Yang, Y. Liu, C. Jia, C. Janiak, N. Tang and X.-J. Yang, *Inorg. Chem.*, 2009, **48**, 10249; E. Redel, C. Röhr and C. Janiak, *Chem. Commun.*, 2009, 2103; E. Redel, M. Fiederle and C. Janiak, *Z. Anorg. Allg. Chem.*, 2009, **635**, 1139; B. Wu, J. Liang, J. Yang, C. Jia, X.-J. Yang, H. Zhang, N. Tang and C. Janiak, *Chem. Commun.*, 2008, 1762; B. Wu, X. Huang, Y. Xia, X.-J. Yang and C. Janiak, *CrystEngComm*, 2007, **9**, 676; T. Dorn, A.-C. Chamayou and C. Janiak, *New J. Chem.*, 2006, **30**, 156; T. Dorn, C. Janiak and K. Abu-Shandi, *CrystEngComm*, 2005, **7**, 633; M. D. Ward, *Chem. Commun.*, 2005, 5838.

27 H. Hosseini Monfared, M. Vahedpour, M. M. Yeganeh, M. Ghorban-loo, P. Mayer and C. Janiak, *Dalton Trans.*, 2011, **40**, 1286–1294; E. Redel, M. Fiederle and C. Janiak, *Z. Anorg. Allg. Chem.*, 2009, **635**, 1139; C. Janiak, A.-C. Chamayou, A. K. M. R. Uddin, M. Uddin, K. S. Hagen and M. Enamullah, *Dalton Trans.*, 2009, 3698–3709; W. Zhang, X. Tang, H. Ma, W.-H. Sun and C. Janiak, *Eur. J. Inorg. Chem.*, 2008, 2830; H. H. Monfared, Z. Kalantari, M.-A. Kamyabi and C. Janiak, *Z. Anorg. Allg. Chem.*, 2007, **633**, 1945; B. Wu, X. Huang, Y. Xia, X.-J. Yang and C. Janiak, *CrystEngComm*, 2007, **9**, 676; B. Wisser, Y. Lu and C. Janiak, *Z. Anorg. Allg. Chem.*, 2007, **633**, 1189; B. Wisser and C. Janiak, *Acta Crystallogr., Sect. E: Struct. Rep. Online*, 2007, **63**, o2871–2872; T. Dorn, C. Janiak and K. Abu-Shandi, *CrystEngComm*, 2005, **7**, 633; K. Abu-Shandi, H. Winkler, H. Paulsen, R. Glaum, B. Wu and C. Janiak, *Z. Anorg. Allg. Chem.*, 2005, **631**, 2705; S. Banerjee, A. Ghosh, B. Wu, P-G. Lassahn and C. Janiak, *Polyhedron*, 2005, **24**, 593; S. Banerjee, B. Wu, P-G. Lassahn, C. Janiak and A. Ghosh, *Inorg. Chim. Acta*, 2005, **358**, 535; C. Zhang, G. Rheinwald, V. Lozan, B. Wu, P-G. Lassahn, H. Lang and C. Janiak, *Z. Anorg. Allg. Chem.*, 2002, **628**, 1259; E. Craven, E. Mutlu, D. Lundberg, S. Temizdemir, S. Dechert, H. Brombacher and C. Janiak, *Polyhedron*, 2002, **21**, 553; X.-J. Yang, F. Drepper, B. Wu, W.-H. Sun, W. Haehnel and C. Janiak, *Dalton Trans.*, 2005, 256 and supplementary material therein.

28 V. A. Blatov and D. M. Proserpio, *Acta Crystallogr., Sect. A: Found. Crystallogr.*, 2009, **65**, 202.

29 The three letter symbols, proposed by M. O'Keeffe, can be retrieved with examples and further information from the Reticular Chemistry Structure Resource database, http://rcsr.anu.edu.au/.

30 Recent NbO topology examples: B. Wang, G.-F. Hou, R.-Q. Meng, L.-H. Bi, B. Li and L.-X. Wu, *CrystEngComm*, 2011, **13**, 1360; B. Zheng, Z. Liang, G. Li, Q. Huo and Y. Liu, *Cryst. Growth Des.*, 2010, **10**, 3405; F. Dai, P. Cui, F. Ye and D. Sun, *Cryst. Growth Des.*, 2010, **10**, 1474; M.-L. Cao, H.-J. Mo and B.-H. Ye, *Cryst. Growth Des.*, 2009, **9**, 546; M. Xue, G. Zhu, Y. Li, X. Zhao, Z. Jin, E. Kang and S. Qiu, *Cryst. Growth Des.*, 2008, **8**, 2478; L Han, W. Zhao, Y. Zhou, X. Li and J. Pan, *Cryst. Growth Des.*, 2008, **8**, 3504.

31 V. A. Blatov, M. O'Keeffe and D. M. Proserpio, *CrystEngComm*, 2010, **12**, 44.

32 http://www.topos.ssu.samara.ru, V. A. Blatov, IUCr Comp-comm. Newsletter, 2006, **7**, 4; http://www.iucr.org/iucr-top/comm/ccom/newsletters.

33 *Chemistry of the Elements*, ed. N. N. Greenwood and A. Earnshaw, 2nd edition. Butterworth, Heinemann, 1997 (p. 982–983).

34 Q.-M. Wang and T. C. W. Mak, *J. Am. Chem. Soc.*, 2001, **123**, 7594; C.-M. Che, M.-C. Tse, M. C. W. Chan, K.-K. Cheung, D. L. Phillips and K.-H. Leung, *J. Am. Chem. Soc.*, 2000, **122**, 2464; M. A. Omary, T. R. Webb, Z. Assefa, G. E. Shankle and H. H. Patterson, *Inorg. Chem.*, 1998, **37**, 1380; N. Schultheiss, D. R. Powell and E. Bosch, *Inorg. Chem.*, 2003, **42**, 5304; A. A. Mohamed, L. M. Pérez and J. P. Fackler Jr., *Inorg. Chim. Acta*, 2005, **358**, 1657; Q.-Y. Lu, Y.-Q. Song, S.-Z. Zhan, J. Cai and J.-P. He, *J. Coord. Chem.*, 2009, **62**(9), 1536; S. Welsch, B. Nohra, E. V. Peresypkina, C. Lescop, M. Scheer and R. Reau, *Chem.–Eur. J.*, 2009, **15**, 4685; D. L. Reger, R. F. Semeniuc, C. A. Little and M. D. Smith, *Inorg. Chem.*, 2006, **45**, 7758; J. C. DeMott, F. Basuli, Uriah J. Kilgore, B. M. Foxman, J. C. Huffman, O. V. Ozerov and D. J. Mindiola, *Inorg. Chem.*, 2007, **46**, 6271.

35 T. Dorn, K. M. Fromm and C. Janiak, *Aust. J. Chem.*, 2006, **59**, 22; X Cheng, T. Liu, X. Duan, F. Wang, Q. Meng and C. Lu, *CrystEngComm*, 2011, **13**, 1314.

36 M. A. Romero, J. M. Salas, M. Quirós, M. P. Sánchez, J. Molina, J. El Bahraoui and R. Faure, *J. Mol. Struct.*, 1995, **354**, 189; J. Elbahraoui, J. Molina and D. Portal, *J. Phys. Chem. A*, 1998, **102**, 2443.

37 *CrystalClearSM 1.4.0*, Rigaku Corporation, Tokyo, Japan. 2007.

38 T. Higashi, *ABSCOR*, Rigaku Corporation, Tokyo, Japan. 1995.

39 *Apex2*, Data Collection Program for the CCD Area-Detector System; SAINT, Data Reduction and Frame Integration Program for the CCD Area-Detector System. Bruker Analytical X-ray Systems, Madison, Wisconsin, USA, 1997–2006.

40 G. M. Sheldrick, *SADABS, Program for area detector adsorption correction*, Institute for Inorganic Chemistry, University of Göttingen, Germany, 1996.

41 A. Altomare, M. C. Burla, M. Camilla, G. L. Cascarano, C. Giacov-azzo, A. Guagliardi, A. G. G. Moliterni, G. Polidori and R. Spagna, *J. Appl. Crystallogr.*, 1999, **32**, 115.

42 G. M. Sheldrick, *Acta Crystallogr., Sect. A: Found. Crystallogr.*, 2008, **64**, 112.

43 A. L. Spek, *J. Appl. Crystallogr.*, 2003, **36**, 7; *PLATON – A Multipurpose Crystallographic Tool*, Utrecht University, Utrecht, The Netherlands, A. L. Spek (2008); Windows implementation: L. J. Farrugia, University of Glasgow, Scotland, Version 40608, 2008.

44 K. Brandenburg, *Diamond (Version 3.2c), Crystal and Molecular Structure Visualization*, Crystal Impact – K. Brandenburg and H. Putz Gbr, Bonn (Germany) 2009.

45 A. D. Becke, *J. Chem. Phys.*, 1993, **98**, 5648.

46 Y. Zhao, N. E. Schultz and D. G. Truhlar, *J. Chem. Theory Comput.*, 2006, **2**, 364.

47 N. Schultz, Y. Zhao and D. G. Truhlar, *J. Phys. Chem. A*, 2005, **109**, 11127.

48 M. J. Frisch, G. W. Trucks, H. B. Schlegel, G. E. Scuseria, M. A. Robb, J. R. Cheeseman, G. Scalmani, V. Barone, B. Mennucci, G. A. Petersson, H. Nakatsuji, M. Caricato, X. Li, H. P. Hratchian, A. F. Izmaylov, J. Bloino, G. Zheng, J. L. Sonnenberg, M. Hada, M. Ehara, K. Toyota, R. Fukuda, J. Hasegawa, M. Ishida, T. Nakajima, Y. Honda, O. Kitao, H. Nakai, T. Vreven, J. A. Montgomery, Jr., J. E. Peralta, F. Ogliaro, M. Bearpark, J. J. Heyd, E. Brothers, K. N. Kudin, V. N. Staroverov, R. Kobayashi, J. Normand, K. Raghavachari, A. Rendell, J. C. Burant, S. S. Iyengar, J. Tomasi, M. Cossi, N. Rega, J. M. Millam, M. Klene, J. E. Knox, J. B. Cross, V. Bakken, C. Adamo, J. Jaramillo, R. Gomperts, R. E. Stratmann, O. Yazyev, A. J. Austin, R. Cammi, C. Pomelli, J. Ochterski, R. L. Martin, K. Morokuma, V. G. Zakrzewski, G. A. Voth, P. Salvador, J. J. Dannenberg, S. Dapprich, A. D. Daniels, O. Farkas, J. B. Foresman, J. V. Ortiz, J. Cioslowski and D. J. Fox, *GAUSSIAN 09 (Revision B.1)*, Gaussian, Inc., Wallingford, CT, 2009.

49 A. Schafer, H. Horn and R. Ahlrichs, *J. Chem. Phys.*, 1992, **97**, 2571.

50 S. Huzinaga and B. Miguel, *Chem. Phys. Lett.*, 1990, **175**, 289.

51 S. Huzinaga and M. Klobukowski, *Chem. Phys. Lett.*, 1993, **212**, 260.

52 W. J. Hehre, R. Ditchfield and J. A. Pople, *J. Chem. Phys.*, 1972, **56**, 2257.

53 R. F. W. Bader, *Atoms in Molecules: A Quantum Theory*, Clarendon Press, Oxford, UK, 1990.

54 R. F. W. Bader, *Chem. Rev.*, 1991, **91**, 893.

55 R. F. W. Bader, in *Encyclopedia of Computational Chemistry*, ed. P. v. R. Schleyer, Wiley, Chichester, UK, 1998.

56 A. D. Becke and K. E. Edgecombe, *J. Chem. Phys.*, 1990, **92**, 5397.

57 B. Silvi and A. Savin, *Nature*, 1994, **371**, 683.

58 S. Noury, X. Krokidis, F. Guster and B. Silvi, *Comput. Chem.*, 1999, **23**, 597.

59 *MORPHY98*, a program written by P. L. A. Popelier, with a contribution from R. G. A. Bone; UMIST, Manchester, U.K., 1998; P. L. A. Popelier, *Comput. Phys. Commun.*, 1996, **93**, 212; P. L. A. Popelier, *Chem. Phys. Lett.*, 1994, **228**, 160.

60 F. Biegler-König, J. Schönbohm and D. Bayles, *J. Comput. Chem.*, 2001, **22**, 545.

61 Jmol: an open-source Java viewer for chemical structures in 3D. http://www.jmol.org/.